Modelling and systematic experimental investigation of mass transfer in supported palladium-based membrane separators

J. Boon **(ECN)**
J.A.Z. Pieterse **(ECN)**
J.W. Dijkstra **(ECN)**
M. van Sint Annaland **(TU/e)**

Modelling and systematic experimental investigation of mass transfer in supported palladium-based membrane separators

Jurriaan Boon[a,b,*], J.A.Z. Pieterse[a], J.W. Dijkstra[a], M. van Sint Annaland[b]

[a]*Sustainable Process Technology, Energy research Centre of the Netherlands, P.O. Box 1, 1755ZG Petten, The Netherlands*
[b]*Multiphase Reactors Group, Department of Chemical Engineering and Chemistry, Eindhoven University of Technology, Den Dolech 2, P.O. Box 513, 5600MB Eindhoven, The Netherlands*

Abstract

Hydrogen separation with palladium-based membranes is considered as a promising technology for pre-combustion CO_2 capture as well as for industrial hydrogen production. With improvements in membrane permeance, resistances to mass transfer are becoming increasingly important. In this work, a systematic approach is followed in order to discern and account for different contributions to the overall mass transfer resistance, based on a combined experimental and modelling approach. Experiments have been performed that started with pure H_2 feed, without sweep, subsequently followed by introducing N_2 on the feed side, and N_2 sweep gas. Using a phenomenological description for the palladium layer and the dusty gas model for the membrane support, coupled to a 2D Navier-Stokes solver with a convection-diffusion equation to account for possible concentration polarisation, all relevant mass transfer resistances are adequately modelled. For the conditions investigated, the main resistances to mass transfer are concentration polarisation in the retentate, hydrogen permeation through the metallic palladium layer, and a diffusional resistance in the support layer.

Keywords: Palladium membrane, Membrane support, Mass transfer resistance, Dusty gas model, Membrane module

[*]Corresponding author: Tel.: +31 224 564576, fax: +31 224 568487.
    Email address: boon@ecn.nl (Jurriaan Boon)

1. Introduction

Metallic palladium foil is permeable only to hydrogen at high temperatures (Graham, 1868) and the industrial potential of palladium membranes was recognised halfway through the 20th century (Darling, 1958). By supporting a thin palladium film on a ceramic support, Uemiya et al. (1988) were able to achieve both a high mechanical strength and a high permeance. Since then, supported palladium and palladium alloy membranes have generated a strong scientific interest, witnessed by a number of reviews (e.g., Shu et al., 1991; Paglieri and Way, 2002; Yun and Oyama, 2011). Nowadays, palladium-based membranes are considered a promising option for hydrogen separation in industrial hydrogen production and in pre-combustion carbon dioxide capture (Metz et al., 2005; Gallucci et al., 2007; Lu et al., 2007; Ockwig and Nenoff, 2007; Basile et al., 2008). With improved stability and permeance figures, testing of palladium-based membranes has evolved to bench scale and even larger scales (Patil et al., 2007; Shirasaki et al., 2009; Li et al., 2010; de Falco et al., 2011; Li et al., 2011; Mahecha-Botero et al., 2011; Li et al., 2012). These tests provide information on membrane performance, but intrinsic membrane characteristics need to be distinguished from module characteristics for a correct interpretation, for scale-up, and also for making a fair comparison among different membranes, and different technologies.

Both the interpretation of experimental results and reliable scale-up strongly depend upon modelling of membranes and membrane modules. Traditionally, the metallic palladium layer has received a great deal of attention. Ward and Dao (1999) have developed detailed rate models for the elementary steps in the permeation of hydrogen through palladium, which have found widespread use. More recently, several authors have added the effects of thermodynamic nonideality (Hara et al., 2009; Flanagan and Wang, 2010; Bhargav et al., 2010). However, with a decrease in palladium thickness and an accompanying increase in flux, other resistances to mass transfer have become increasingly more important, viz. concentration polarisation and the mass transfer resistance in the membrane support. Concentration polarisation refers to the occurrence of concentration gradients in the gas phase near the membrane surface and is affected by the gas flow conditions in the membrane module, rather than of the processes inside the membrane itself. In a modelling study, Tiemersma et al. (2006) have shown the importance of concentration polarisation in a packed bed membrane reactor with high-flux membranes. In an experimental study, systematically introducing inert, Peters et al. (2008) have also demonstrated the importance of concentration polarisation for supported palladium-based membrane separators. With experiments and

modelling, Nair and Harold (2008) have shown the impact of temperature, pressure, and hydrogen concentration upon concentration polarisation. Catalano et al. (2009) have modelled the mass transfer resistance in the module gas phase with an overall mass transfer coefficient. Boon et al. (2011) indicated the importance of the drift flux for radial hydrogen transport and the need for 2D modelling of the membrane module. Mass transfer resistance in the membrane support has been studied by Goto et al. (2000), Gabitto and Tsouris (2008), and Iwuchukwu and Sheth (2008), introducing expressions for Knudsen flow and viscous bulk flow through the support matrix of supported palladium membranes. Caravella et al. (2008), in a modelling study, were the first to introduce the dusty gas model (Krishna and Wesselingh, 1997) to account for Knudsen and viscous flow as well as molecular diffusion in the support. Bhargav et al. (2010) combined the effect of the nonideality of the H-Pd system with a dusty gas model description of the membrane support. With an experimental and modelling approach, they demonstrated that the bulk and surface processes in the palladium metal are dominant at temperatures below 300°C, whereas the resistance in the porous substrate becomes important at higher temperatures. However, their study did not include the effect of sweep gas at the permeate side, while such a condition can add an additional diffusional resistance according to the dusty gas model, and is extremely relevant from an industrial point of view.

In conclusion, three major contributions to the transfer of hydrogen across the membrane from the feed gas to the permeate can be discerned:

1. gas phase convection and diffusion in the module (retentate and permeate side),

2. hydrogen permeation across the metallic palladium layer, and

3. transfer of hydrogen across the membrane support.

In this paper, a systematic approach is followed to study these steps, schematically depicted in Figure 1. Experiments have been carried out in three parallel single membrane modules, starting with pure hydrogen feed without sweep, followed by the introduction of nitrogen on the feed side which increases mass transfer resistances, and finally use nitrogen sweep gas. To interpret the experimental data, a model is developed for the membrane module. Starting with a phenomenological description for the palladium layer, a 2D model has been introduced for convection and diffusion in the module and the dusty gas model is used to describe the mass transport in the porous support. The model has subsequently been used to
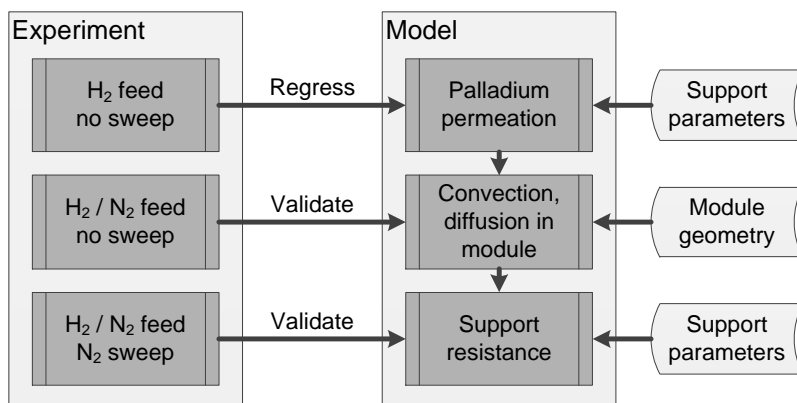
Figure 1: Research strategy, systematically performing experiments to develop parts of the model

study the relative importance of the phenomena mentioned above, thereby allowing to discern intrinsic effects of the membrane from external (module) effects — a crucial step in the interpretation of the experimental results and for validation of the model for the membrane module required for reliable scale-up.

The paper is organised as follows: first, the experimental test-rig and experimental conditions are outlined, followed by a description of the model, then experimental and modelling results are presented and discussed, highlighting the key mass transfer resistances in the hydrogen separation process.

2. Experimental

2.1. Membranes and modules

Membranes were obtained from Hysep (the Netherlands). They consist of a thin (3–9 μm) layer of palladium on a ceramic support tube, as shown in Figure 2 (Hysep, 2012). The support tubes are ceramic tubes of 14 mm outer diameter and 2 mm thickness and contain three layers of different structure. The properties of the support tube layers have been summarised in Table 1. Three membranes have been used in a parallel configuration. After sealing (Rusting et al., 2001), the effective length of each of the membranes is approximately 45 cm, giving a total surface area for three membranes of 595 cm^2.

Each of the membrane tubes was mounted in a cylindrically shaped module (see Figure 3). An insert tube is used for the sweep gas, creating a double annulus geometry enclosing the membrane. The use of multiple membranes serves to achieve suitable total membrane surface areas for the workable flow ranges of the
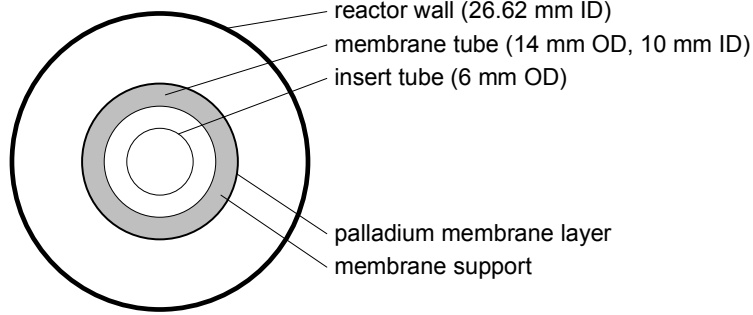
Figure 2: Membrane geometry

Layer	Thickness	ϵ	d_{pore} [a]	τ [b]	B_0 [c]	$\mathcal{D}^{e}_{H_2,M}$ [d]	$\mathcal{D}^{e}_{N_2,M}$ [d]
	μm		nm		10^{-15} m^2	10^{-4} m^{2}s^{-1}	10^{-4} m^{2}s^{-1}
1	2000	0.43	3400	1.25	124	10.4	2.78
2	30–50	0.35	160	1.25	0.224	0.397	0.107
3	30–50	0.35	160	1.25	0.224	0.397	0.107

[a] Approximate mean pore diameter

[b] Estimate

[c] Calculated from equation 5

[d] Calculated from equation 4

Table 1: Membrane support parameters for the three α-Al$_2$O$_3$ layers

test rig. In these conditions, the Reynolds number varies up to a maximum of 1100, assuring laminar flow conditions in all experiments.

2.2. Test procedure

Experiments on pure H$_2$ permeance and H$_2$-N$_2$ separation have been performed on ECN's 'Process Development Unit' (PDU), described in more detail elsewhere (Jansen et al., 2009; Li et al., 2011). The modules were placed in an electrically heated oven at 400°C, with a maximum temperature gradient over the module length of 25°C. H$_2$ and N$_2$ were fed by Bronkhorst (the Netherlands) mass flow controllers, listed in Table 2. Gas distribution over the three modules was controlled by orifices and uniform. The pressures on the retentate and permeate side were controlled by a back pressure control (Bronkhorst) and measured at the module outlets with a pressure transducer (Swagelok, USA). Data with a deviation between pressure control and measurement of more than 10% of the pressure dif-
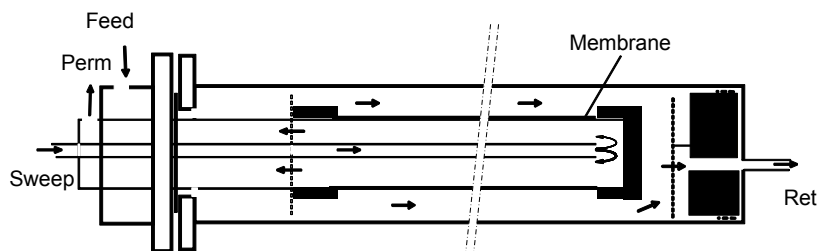
Figure 3: Cross-section of the PDU membrane module

Gas	Min	Max	
H_2	0.2	10	Nl min^{-1}
H_2 - flow sensor	1	200	Nl min^{-1}
N_2 feed	0.7	35	Nl min^{-1}
N_2 sweep	1.7	85	Nl min^{-1}

Table 2: PDU flow controllers

ference over the membrane were discarded. The gas flow rate in the retentate and permeate has been measured by mass flow meters (Bronkhorst). The gas composition of the total retentate and permeate flows as well as that of the stream exiting the individual membrane tubes was determined with a gas chromatograph (HP, P200H) equipped with a molsieve column, a Poraplot column and a TCD detector. In addition, an Advance Optima online analysis (ABB Magnos106) was used to monitor the concentration of H_2 with a Caldos 4T-EX detector. Process values have been recorded when for five minutes the pressures were stable (±5 kPa) and the measured flows were stable (±0.03 Nl min^{-1}), and the measurements have been repeated three times. H_2 and N_2 mass balance assessments with representative gas mixtures during test runs have shown to be mostly within $\pm5\%$. Incidental measurements with a mass balance error more than $\pm7\%$ have been discarded.

After a leak test at room temperature the membranes have been purged with N_2 on the feed and permeate side to remove air from the system. Subsequently, the reactor was heated to 400°C with a ramp of 1°Cmin^{-1} while applying a N_2 flow at the feed and sweep side, followed by a pure N_2 leak test. With a retentate pressure of 0.6 MPa and a permeate pressure of 0.11 MPa, a leak rate of 0.02 Nl min^{-1} was found. After the separation tests, the N_2 leak test was repeated at 0.6 MPa and 0.15 MPa, yielding a leak rate of 0.20 Nl min^{-1}. Although there is a small increase in the leak rate, a high selectivity is maintained throughout the experiments and a correction of the experimental results for leak flow was therefore not necessary.

6

After the first leak test at 400°C, the feed and permeate side were purged with 20 Nl min^{-1} of H$_2$ for 30 minutes in order to remove the remaining N$_2$, followed by a stabilisation period of 23 hours in 0.21/0.11 MPa of H$_2$ (20 Nl min^{-1} of H$_2$ on the feed side, no sweep) and measurement of the pure H$_2$ permeance of the membranes every two hours. After stabilisation, pure H$_2$ permeance tests were done at 400°C. Then gas mixtures of 55% H$_2$ in N$_2$ were tested, varying retentate and permeate pressures, feed flow and sweep flow rates. To make sure no trends would be induced by the measurement history, the order of the experiments was randomised.

3. Modelling

A model has been developed for the interpretation of the role of the different mass transfer resistances in the experiments. Inside the membrane itself, the palladium layer and the support layers are mass transfer resistances in series. Laminar convection and diffusion, i.e. concentration polarisation, in the module are accounted for by solving the mass and momentum balances, assuming 2D axial symmetry.

3.1. Membrane

3.1.1. Palladium

The mechanisms by which H$_2$ crosses the metallic palladium separation layer are complex and their modelling is inherently challenging. A number of sequential steps may be discerned according to Ward and Dao (1999):

- dissociative adsorption of H$_2$ on the Pd surface at the retentate side,

- transition of H atoms from the surface into the Pd bulk,

- diffusion through the bulk,

- transition of H atoms from the bulk to the Pd surface at the permeate side, and

- recombinative desorption from the metal surface.

The individual steps have very different kinetics, and the overall kinetics depend on their relative importance. Ward and Dao (1999) have made a detailed model for each of the steps and concluded that the diffusion of H atoms through the Pd bulk is rate-limiting, at least for a clean Pd layer with a thickness down to 1 μm

7

and temperatures above 300°C. In such a case, overall kinetics will obey Sieverts'
law,

$$N_{\mathrm{m}} = Q(T)\left(p_{\mathrm{H_2,r}}^{n} - p_{\mathrm{H_2,p}}^{n}\right) \tag{1}$$

with $n = 0.5$ (Sieverts and Krumbhaar, 1910). Here, N_{m} is the transmembrane
flux, defined at the radial coordinate of the palladium layer (r_{m}), $Q(T)$ is the
temperature-dependent permeance, $p_{\mathrm{H_2,r}}$ and $p_{\mathrm{H_2,p}}$ are the retentate-side and permeate-
side H_2 partial pressures, respectively. Later authors have added that, at higher
H_2 partial pressures, corrections for the nonideality of the H-Pd system, surface
effects, or thermal effects will lead to increased values of n (Hara et al., 2009;
Flanagan and Wang, 2010; Bhargav et al., 2010; Skorpa et al., 2012). For the pur-
pose of the present study, it is sufficient to fit the parameters Q and n in equation
(1) to experimental pure H_2 permeation data.

3.1.2. Membrane support

After H_2 molecules desorb from the metallic palladium separation layer on
the permeate side, they need to cross the porous ceramic support layer before
they end up in the permeate stream. The driving forces for the transfer of H_2
across the support are gradients in mole fraction and pressure. These driving
forces are balanced by the friction forces exerted by gas molecules and the porous
medium, which can be described by the dusty gas model (DGM), taking into
account viscous flow, Knudsen diffusion, and molecular diffusion (Mason and
Lonsdale, 1990; Krishna and Wesselingh, 1997). For radial transport of N_{sp} ideal
gas species i in an isothermal system, in absence of significant body forces,

$$\sum_{j=1}^{N_{\mathrm{sp}}} \frac{y_j N_i - y_i N_j}{\mathcal{D}_{ij}^{\mathrm{e}}} + \frac{N_i}{\mathcal{D}_{i\mathrm{M}}^{\mathrm{e}}} = -\frac{p}{RT}\frac{dy_i}{dr} - \frac{y_i}{RT}\left(1 + \frac{B_0 p}{\mu \mathcal{D}_{i\mathrm{M}}^{\mathrm{e}}}\right)\frac{dp}{dr} \tag{2}$$

where y_i is the mole fraction of i, p the total pressure, R the gas constant, and r
the radial coordinate. The remaining transport coefficients are:
$\mathcal{D}_{i,j}^{\mathrm{e}}$ the effective binary Maxwell-Stefan gas-gas diffusivity in the porous matrix,
$\mathcal{D}_{i\mathrm{M}}^{\mathrm{e}}$ the effective binary Knudsen diffusivity, with respect to the matrix, and
B_0 the viscous permeability of the support matrix.
The effective Maxwell-Stefan diffusivity is given by (Krishna and Wesselingh,
1997):

$$\mathcal{D}_{ij}^{\mathrm{e}} = \frac{\epsilon}{\tau}\mathcal{D}_{ij} \tag{3}$$

where ϵ and τ are the support porosity and tortuosity, respectively. For an ideal gas
the Maxwell-Stefan diffusivity ($\mathcal{D}_{ij}$) equals the Fick diffusivity (D_{ij}) (Taylor and

Krishna, 1993). The Knudsen diffusivity is given by (Krishna and Wesselingh, 1997):

$$\mathcal{D}_{i\mathrm{M}}^{\mathrm{e}} = \frac{\epsilon}{\tau} \frac{d_{\mathrm{pore}}}{3} \sqrt{\frac{8RT}{\pi M_i}} \tag{4}$$

where d_{pore} is the pore diameter and M_i is the molar mass of species i. If convection through the support is modelled as laminar, incompressible flow through cylindrical pores, the Hagen-Poiseuille law with added porosity and tortuosity modification gives (Bird et al., 1960; Krishna and Wesselingh, 1997):

$$B_0 = \frac{\epsilon}{\tau} \frac{d_{\mathrm{pore}}^2}{32} \tag{5}$$

The current system comprises a maximum of two species on the permeate side of the membrane: H_2 and a non-permeating sweep gas species (N_2). Since $y_{H_2} + y_{N_2} = 1$, $dy_{N_2}/dr = -dy_{H_2}/dr$, and with use of the equation of continuity ($d(rN_i)/dr = 0$),

$$\frac{dp}{dr} = \frac{r_{\mathrm{m}}N_{\mathrm{m}}}{r\mathcal{D}_{1\mathrm{M}}^{\mathrm{e}}} \left[-\frac{y_{H_2}}{RT}\left(1 + \frac{B_0 p}{\mu \mathcal{D}_{1\mathrm{M}}^{\mathrm{e}}}\right) - \frac{1 - y_{H_2}}{RT}\left(1 + \frac{B_0 p}{\mu \mathcal{D}_{2\mathrm{M}}^{\mathrm{e}}}\right) \right]^{-1} \tag{6}$$

$$\frac{dy_{H_2}}{dr} = -\frac{y_{H_2}}{p}\left(1 + \frac{B_0 p}{\mu \mathcal{D}_{1\mathrm{M}}^{\mathrm{e}}}\right)\frac{dp}{dr} - \frac{r_{\mathrm{m}}N_{\mathrm{m}}RT}{rp}\left(\frac{1}{\mathcal{D}_{1\mathrm{M}}^{\mathrm{e}}} + \frac{1 - y_{H_2}}{\mathcal{D}_{12}^{\mathrm{e}}}\right) \tag{7}$$

The coupled differential equations (6–7) are solved with a variable order Adams-Bashforth-Moulton method in Matlab with built-in solver *ode113* from $r = r_{\mathrm{mi}}$ (where y_{H_2} and p are known) to $r = r_{\mathrm{m}}$. The derivation elucidates two distinct mechanisms that add to the resistance of H_2 transport across the support layers: a molecular friction resistance as expressed by dy_{H_2}/dr and a support friction resistance expressed by dp/dr.

3.2. Membrane module

Both the feed/retentate side and the countercurrent sweep/permeate side of the module have an annular shape. For description of fluid flow and mass transfer, 2D steady state isothermal differential mass and momentum balances are solved for both channels in cylindrical geometry. The gas density is evaluated locally but its derivatives are ignored. The equations of continuity and motion, and the H_2 material balance in a mixture with a single inert component reduce to (Bird et al.,

9

1960):

$$\frac{\rho}{r}\frac{\partial}{\partial r}(rv_r) + \rho\frac{\partial v_z}{\partial z} = 0 \tag{8}$$

$$\rho v_r\frac{\partial v_z}{\partial r} + \rho v_z\frac{\partial v_z}{\partial z} = -\frac{\partial p}{\partial z} + \frac{\mu}{r}\frac{\partial}{\partial r}\left(r\frac{\partial v_z}{\partial r}\right) + \mu\frac{\partial^2 v_z}{\partial z^2} \tag{9}$$

$$v_r\frac{\partial c_{H_2}}{\partial r} + v_z\frac{\partial c_{H_2}}{\partial z} = \frac{D}{r}\frac{\partial}{\partial r}\left(r\frac{\partial c_{H_2}}{\partial r}\right) + D\frac{\partial^2 c_{H_2}}{\partial z^2} \tag{10}$$

$$\frac{\partial}{\partial r}\left(\frac{\partial p}{\partial z}\right) = 0 \tag{11}$$

Here, z is the axial coordinate, ρ the gas density, μ the gas viscosity, D the gas diffusivity of H_2, and c the concentration. The boundary conditions are no-slip at the module walls,

$$v_z|_{r=r_{si}} = v_z|_{r=r_{so}} = v_z|_{r=r_m} = v_z|_{r=r_r} = 0 \tag{12}$$

(r_{si} and r_{so} are the inner and outer radii of the sweep channel and r_r is inner diameter of the surrounding module wall) except for the radial velocity at the membrane surface:

$$v_r|_{r=r_m} = N_m\frac{RT}{p} \tag{13}$$

$$v_r|_{r=r_{so}} = \frac{N_m r_m}{r_{so}}\frac{RT}{p} \tag{14}$$

$$\left(v_r c_{H_2} - D_{H_2}\frac{\partial c_{H_2}}{\partial r}\right)\bigg|_{r=r_m} = N_m \tag{15}$$

$$\left(v_r c_{H_2} - D_{H_2}\frac{\partial c_{H_2}}{\partial r}\right)\bigg|_{r=r_{so}} = \frac{N_m r_m}{r_{so}} \tag{16}$$

At the inlets, developed laminar flow velocity profiles have been assumed (Bird et al., 1960, §2.4).

Four dependent variables v_r, v_z, c_{H_2}, and $\partial p/\partial z$ are determined by the coupled partial differential equations (8–11) that have been solved as ordinary differential equations in Matlab by collocation with built-in solver *bvp4c* after discretisation in finite differences for z, using second-order upwind approximation for the convection terms and a centered-space approximation for the diffusion terms (Hoffman, 2001). The mixing-cup average flow and concentration are obtained

Parameter	Estimate	Estimated error	Unit	t Statistic
Q	$1.54 \cdot 10^{-4}$ ±	$0.16 \cdot 10^{-4}$	mol m^{-2} s^{-1} Pa$^{-0.730}$	19.4
n	0.730 ±	0.007		211
N_{data}	43			

Error estimate with 95% confidence interval

Table 3: Regressed membrane flux equation (1) parameters at 400°C

by trapezoidal integration afterwards, to derive experimentally determined process quantities, such as the outlet flow rate and H_2 concentration for the retentate and permeate.

Initial experiments have been done with only H_2 on both sides of the membrane, i.e. with a pure H_2 feed and without sweep gas, in which case the module model can be greatly simplified. Assuming a negligible pressure drop both in the axial and in the radial direction, the local H_2 pressure is equal to the measured retentate or permeate pressure. The H_2 pressure in the flux equation (equation 1) can then be evaluated directly and the solution of the module hydrodynamics can be omitted.

4. Results

4.1. Hydrogen feed, no sweep

Pure H_2 experiments without sweep were done for the determination of the parameters in equation (1). Retentate and permeate pressures were varied in the range of 0.24–3.3 MPa, and 0.11–3.0 MPa, respectively. The pressure difference over the membrane was varied between 0.10 MPa and 0.38 MPa. H_2 fluxes were measured in the range of 0.22–0.85 mol m^{-2} s^{-1}.

Using nonlinear regression, the permeation equation (1), and the support pressure drop equation (6), values for Q and n were determined as shown in Table 3. The statistics show the relevance and the accuracy of the model parameters. The equation fits the data points well as shown in Figure 4. The maximum pressure drop over the support layer as predicted with the DGM was 13.5 kPa. For these conditions, the predicted H_2 flux across the membrane in absence of a pressure drop over the support layer would be 3% higher than the current flux prediction. For ease of comparison with literature reports, the same procedure with $n = 1$ was used to determine a linearised permeance of $2.5 \cdot 10^{-6}$ mol m^{-2} s^{-1} Pa^{-1}.
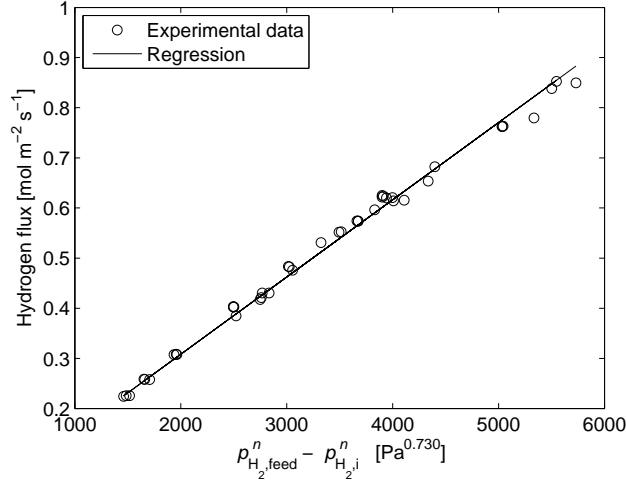
Figure 4: Measured and regressed H_2 flux versus driving force; pure H_2, no sweep

4.2. Hydrogen-nitrogen feed

Gas mixtures of 55% H_2 in N_2 were fed to the membranes at 3.0 MPa retentate pressure. The permeate side was controlled at 0.39–2.0 MPa, both without sweep gas and with 3–60 Nl min^{-1} of N_2 sweep. During all experiments, the feed flow was adjusted in the range of 20–80 Nl min^{-1} in order to have a H_2 recovery of 20–90%.

The model was run in four modes, shown in Table 4. First, the model was run with gas phase convection and diffusion, but without accounting for mass transfer resistance in the support, which implies $dp/dr = 0$ and $dy_{H_2}/dr = 0$ in equations (6–7) and leaving out the DGM altogether. The flux is then based directly upon the partial pressure difference between retentate and permeate sides. In mode II and III, respectively, the resistances by pressure drop and diffusion were included. Finally, in mode IV, the full DGM was included for the membrane support, accounting for both the diffusional resistance and the pressure drop. Parity plots of the results for modes I and IV versus measured fluxes are shown in Figure 5. The quality of the match between model prediction and measured H_2 flux is expressed as the average absolute relative deviation, shown in the last column of Table 4.

With the complete model in mode IV, four different conditions have been simulated: pure H_2 feed without sweep, H_2-N_2 feed without sweep, H_2-N_2 feed with low sweep flow rate, and H_2-N_2 feed with high sweep flow rate. For these conditions, radial H_2 concentration profiles at three axial positions are shown in Fig-

ures 6–9. Figure 6 shows the H_2 concentration profiles for pure H_2 feed without sweep at 0.3 MPa retentate and 0.1 MPa permeate pressure. Only one axial position (225 mm) is plotted because there are no axial gradients in the module. The pressure drop over the support layer, in this case 14 kPa, is the only mass transfer resistance apart from the palladium layer and it results in a slight increase of the H_2 concentration over the support layer. Next, three H_2-N_2 cases were simulated for 3.0 MPa retentate and 1.1 MPa permeate pressure. Figure 7 shows the H_2 concentration profiles for H_2-N_2 feed without sweep. The pressure drop in the membrane support is no longer significant. Clearly, the presence of inert N_2 on the feed side induces additional mass transfer resistance, leading to a marked decrease in H_2 flux. Firstly, in the radial direction, concentration polarisation strongly reduces the H_2 concentration at the membrane surface. Secondly, as H_2 permeates through the membrane, the feed side becomes H_2 depleted as evidenced from the decrease of the average H_2 concentration with the axial position. In Figure 7, the retentate side concentration at 435 mm, i.e. near the retentate outlet, closely approaches the permeate side concentration and the driving force for H_2 permeation becomes small while the retentate still contains most of the H_2 that was present in the feed. The length-averaged H_2 flux at the membrane surface is -0.26 mol m^{-2} s^{-1}. Figure 8 and Figure 9 show the H_2 concentration profiles for H_2-N_2 feed with 3 Nl min^{-1}, and 50 Nl min^{-1} sweep, respectively. The benefit of using sweep gas is clearly evident from the lower H_2 concentration near the retentate outlet. In fact, the mixing-cup average H_2 concentrations in the retenate are 142 mol m^{-3} and 91 mol m^{-3}, and the length-averaged H_2 fluxes at the membrane surface are -0.37 mol m^{-2} s^{-1} and -0.44 mol m^{-2} s^{-1}, respectively. On the other hand, the permeate side mixing-cup H_2 concentrations of 166 mol m^{-3} and 80 mol m^{-3}, respectively, show a marked decrease with increasing with sweep flow rate. Also, Figure 8 and Figure 9 show that two additional resistances to mass transfer become significant. A small radial concentration gradient over the permeate indicates concentration polarisation. More importantly, a concentration gradient is formed over the support layer which is caused by penetration of the support by sweep gas, forming a diffusion barrier to H_2 transfer.

5. Discussion

5.1. Permeation model

After correction for pressure drop in the support, the permeation parameters have been determined for the palladium layer as shown in Table 3. The value of n = 0.730 ± 0.007 is in line with values reported in literature for similar
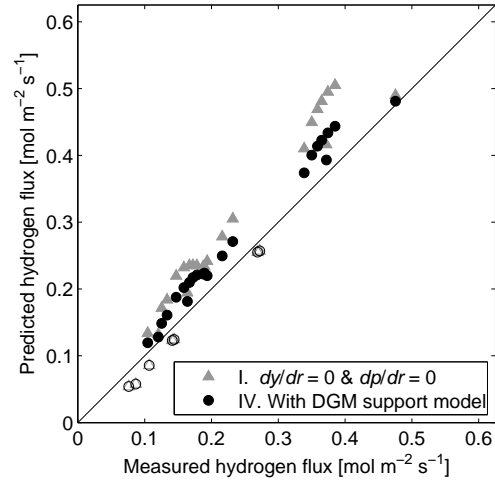
Figure 5: Parity plot of predicted versus measured flux with H_2-N_2 feed, N_2 sweep; modes as defined in Table 4, open symbols no sweep, closed symbols with N_2 sweep

Mode	Pd model	Support model		Module model	Mean absolute deviation
		dp/dr	dy_{H_2}/dr		$\langle |(\mathbf{N}_m^{pred} - \mathbf{N}_m^{meas})/\mathbf{N}_m^{meas}| \rangle$
I	Eq. 1	0	0	Eqns. 8–11	26.0%
II	Eq. 1	Eq. 6	0	Eqns. 8–11	25.9%
III	Eq. 1	0	Eq. 7	Eqns. 8–11	16.5%
IV	Eq. 1	Eq. 6	Eq. 7	Eqns. 8–11	16.6%

Table 4: Comparison of predicted fluxes with measured fluxes for H_2-N_2 separation cases

14
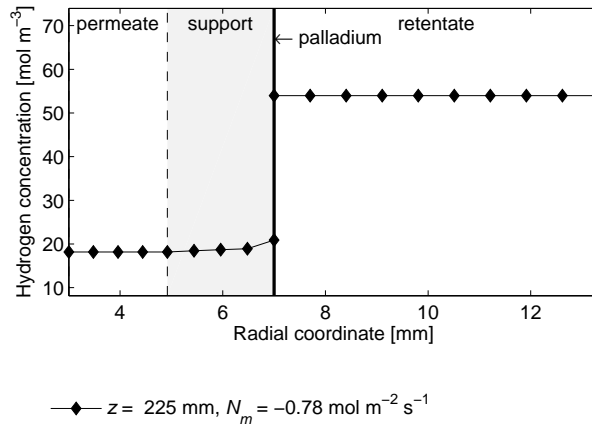
Figure 6: Radial H_2 concentration profile for pure H_2 feed, no sweep (80 Nl min^{-1} feed 100% H_2, retentate pressure 0.3 MPa, permeate pressure 0.1 MPa, measured flux -0.76 mol m^{-2} s^{-1})
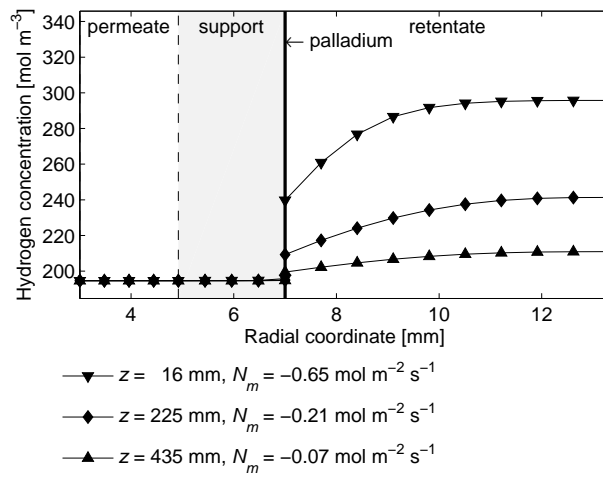

Figure 7: Radial H_2 concentration profiles, H_2/N_2 feed, no sweep (78 Nl min^{-1} feed 55% H_2, retentate pressure 3.0 MPa, permeate pressure 1.1 MPa, measured flux -0.27 mol m^{-2} s^{-1})
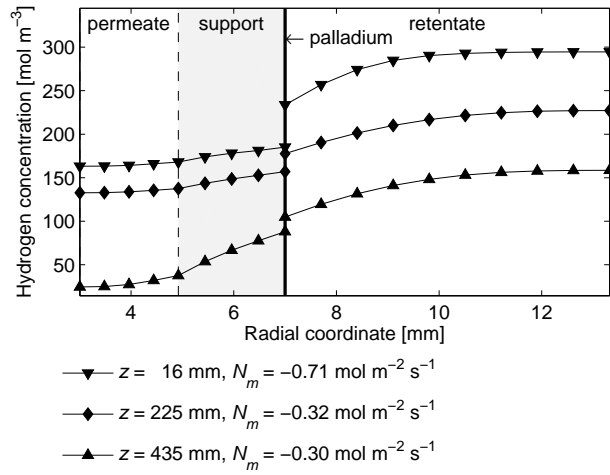
Figure 8: Radial H_2 concentration profiles, H_2/N_2 feed, 5.0 Nl min^{-1} sweep (78 Nl min^{-1} feed 55% H_2, retentate pressure 3.0 MPa, permeate pressure 1.1 MPa, measured flux -0.34 mol m^{-2} s^{-1})
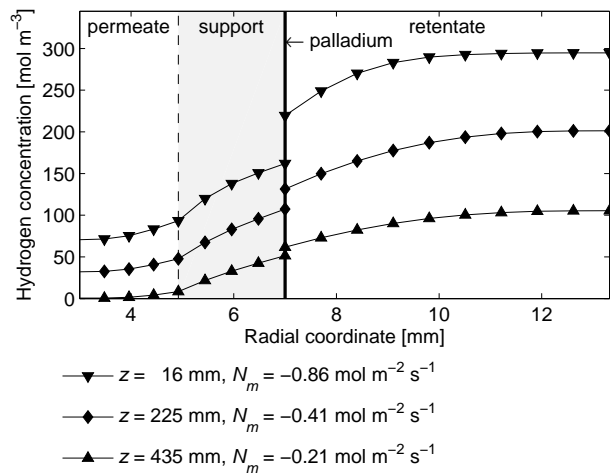
Figure 9: Radial H_2 concentration profiles, H_2/N_2 feed, 50 Nl min^{-1} sweep (78 Nl min^{-1} feed 55% H_2, retentate pressure 3.0 MPa, permeate pressure 1.1 MPa, measured flux -0.39 mol m^{-2} s^{-1})

membranes and conditions (Rothenberger et al., 2004; Yun and Oyama, 2011). The permeation equation (1) fits the data well. With a linearised permeance of $2.5 \cdot 10^{-6}$ mol m^{-2} s^{-1} Pa^{-1}, the H$_2$ permeance of the Hysep membranes ranks among the higher permeabilities reported in literature (Yun and Oyama, 2011). The model predicted pressure drop over the support layer in the pure H$_2$ experiments is relatively small, at a maximum of 13.5 kPa. The difference in flux caused by the pressure drop in the support amounts to only 3% and the pressure drop over the support layer could be ignored in assessing the pure H$_2$ measurements.

5.2. *Mass transfer resistance in the membrane support*

Four simulation modes were used, with different parts of the DGM to account for mass transfer resistance in the membrane support. A combination of the permeation model with the 2D module model in mode I already gives good results for the cases without sweep gas (Figure 5). Clearly, both concentration polarisation in the module and permeation through the membrane are accurately predicted. In contrast, the model predictions in mode I do not represent the measurements with N$_2$ sweep. Including pressure drop over the membrane support in mode II slightly improves the match, but a much greater improvement is made in mode III, when the diffusional resistance by N$_2$ in the membrane support is included. Finally, the permeation model combined with the 2D module model and the support resistance model based on the DGM (mode IV) gives a prediction of the experimentally measured flux for all cases with an average error of 16.6%. Based on a comparison of the predicted fluxes with measured fluxes for the entire dataset (Table 4), it can be concluded that the largest contribution of the support resistance for these experimental conditions results from the diffusional resistance due to penetration of sweep gas into the support. The effect of the resistance by the support matrix is negligible.

Inspection of the H$_2$ concentration profiles in the module clearly highlights the need for using a sweep gas in order to obtain a feasible recovery. The remaining H$_2$ concentration in the retentate outlet, and of course the obtained H$_2$ concentration in the permeate as well, is a strong function of the sweep flow rate. But apart from the effect upon the overall driving force, the introduction of sweep gas induces an increased resistance to mass transfer. For the cases studied, the overall resistance to H$_2$ transfer from retentate to permeate is formed mainly by concentration polarisation on the feed side, permeation across the palladium layer, and the diffusion barrier created by penetration of sweep gas in the membrane support. The feasible amount of sweep gas in any practical application must be determined

based on the overall process, and by accounting for concentration polarisation, permeation through the palladium, and membrane support resistance.

6. Conclusion

The strategy presented, consisting of matching results from experiments and model development, has proven to be a valuable tool in benchmarking membrane performance. The model can also be used for predicting membrane performance at commercial scale. Using experiments with pure hydrogen feed and no sweep, the permeation of hydrogen through the metallic palladium layer was accurately fitted with a standard permeation equation (1) with Q and n as regressed parameters. The pressure drop in the membrane support was included but was found to be very small. Hydrogen-nitrogen separation experiments without sweep gas could be predicted by a 2D laminar flow convection and diffusion model. Thus, convective and diffusive transport of hydrogen and inert in the modules was successfully accounted for by the module model. Experiments with nitrogen sweep gas have shown significant resistances in the membrane support. These were predicted by the dusty gas model to be both a small pressure drop and a rather large mole fraction gradient in the support layer, the latter being far more important than the former. The derived model allows to quantify, as a function of operating conditions, the intrinsic and external mass transfer resistances.

References

Basile, A., Gallucci, F., Tosti, S., 2008. Synthesis, characterization, and applications of palladium membranes, in: Mallada, R., Menéndez, M. (Eds.), Inorganic Membranes: Synthesis, Characterization and Applications. Elsevier. volume 13 of *Membrane Science and Technology*, pp. 255–323.

Bhargav, A., Jackson, G., Ciora, R., Liu, P., 2010. Model development and validation of hydrogen transport through supported palladium membranes. Journal of Membrane Science 356, 123–132.

Bird, R.B., Stewart, W.E., Lightfoot, E.N., 1960. Transport Phenomena. Wiley, New York.

Boon, J., Li, H., Dijkstra, J.W., Pieterse, J.A.Z., 2011. 2-dimensional membrane separator modelling: Mass transfer by convection and diffusion. Energy Procedia 4, 699–706.

Caravella, A., Barbieri, G., Drioli, E., 2008. Modelling and simulation of hydrogen permeation through supported Pd-alloy membranes with a multicomponent approach. Chemical Engineering Science 63, 2149–2160.

Catalano, J., Baschetti, M.G., Sarti, G.C., 2009. Influence of the gas phase resistance on hydrogen flux through thin palladium-silver membranes. Journal of Membrane Science 339, 57–67.

Darling, A., 1958. The diffusion of hydrogen through palladium. Platinum Metals Review 2, 16–22.

de Falco, M., Iaquaniello, G., Salladini, A., 2011. Experimental tests on steam reforming of natural gas in a reformer and membrane modules (RMM) plant. Journal of Membrane Science 368, 264–274.

Flanagan, T.B., Wang, D., 2010. Exponents for the pressure dependence of hydrogen permeation through Pd and Pd-Ag alloy membranes. Journal of Physical Chemistry C 114, 14482–14488.

Gabitto, J., Tsouris, C., 2008. Hydrogen transport in composite inorganic membranes. Journal of Membrane Science 312, 132–142.

Gallucci, F., Basile, A., Drioli, E., 2007. Methanol as an energy source and/or energy carrier in membrane processes. Separation & Purification Reviews 36, 175–202.

Goto, S., Assabumrungrat, S., Tagawa, T., Praserthdam, P., 2000. The effect of direction of hydrogen permeation on the rate through a composite palladium membrane. Journal of Membrane Science 175, 19–24.

Graham, T., 1868. On the relation of hydrogen to palladium. Proceedings of the Royal Society of London 17, 212–220.

Hara, S., Ishitsuka, M., Suda, H., Mukaida, M., Haraya, K., 2009. Pressure-dependent hydrogen permeability extended for metal membranes not obeying the square-root law. The Journal of Physical Chemistry B 113, 9795–9801.

Hoffman, J.D., 2001. Numerical Methods for Engineers and Scientists. Taylor & Francis, Boca Raton. 2nd edition.

Hysep, 2012. Hydrogen separation modules. http://www.hysep.com/. Accessed 22 February.

Iwuchukwu, I.J., Sheth, A., 2008. Mathematical modeling of high temperature and high-pressure dense membrane separation of hydrogen from gasification. Chemical Engineering and Processing: Process Intensification 47, 1298–1310.

Jansen, D., Dijkstra, J.W., Van den Brink, R.W., Peters, T.A., Stange, M., Bredesen, R., Goldbach, A., Xu, H.Y., Gottschalk, A., Doukelis, A., 2009. Hydrogen membrane reactors for CO_2 capture. Energy Procedia 1, 253–260.

Krishna, R., Wesselingh, J.A., 1997. The Maxwell-Stefan approach to mass transfer. Chemical Engineering Science 52, 861–911.

Li, H., Dijkstra, J.W., Pieterse, J.A.Z., Boon, J., van den Brink, R.W., Jansen, D., 2010. Towards full-scale demonstration of hydrogen-selective membranes for CO_2 capture: Inhibition effect of WGS-components on the H_2 permeation through three Pd membranes of 44 cm long. Journal of Membrane Science 363, 204–211.

Li, H., Pieterse, J.A.Z., Dijkstra, J.W., Boon, J., van den Brink, R.W., Jansen, D., 2012. Bench-scale WGS membrane reactor for CO_2 capture with co-production of H_2. International Journal of Hydrogen Energy 37, 4139–4143.

Li, H., Pieterse, J.A.Z., Dijkstra, J.W., Haije, W.G., Xu, H.Y., Bao, C., Van den Brink, R.W., Jansen, D., 2011. Performance test of a bench-scale multi-tubular membrane reformer. Journal of Membrane Science 373, 43–52.

Lu, G.Q., Diniz da Costa, J.C., Duke, M., Giessler, S., Socolow, R., Williams, R.H., Kreutz, T., 2007. Inorganic membranes for hydrogen production and purification: A critical review and perspective. Journal of Colloid and Interface Science 314, 589–603.

Mahecha-Botero, A., Boyd, T., Gulamhusein, A., Grace, J.R., Lim, C.J., Shirasaki, Y., Kurokawa, H., Yasuda, I., 2011. Catalytic reforming of natural gas for hydrogen production in a pilot fluidized-bed membrane reactor: Mapping of operating and feed conditions. International Journal of Hydrogen Energy 36, 10727–10736.

Mason, E.A., Lonsdale, H.K., 1990. Statistical-mechanical theory of membrane transport. Journal of Membrane Science 51, 1–81.

Metz, B., Davidson, O., de Coninck, H., Loos, M., Meyer, L. (Eds.), 2005. IPCC special report on Carbon Dioxide Capture and Storage. Cambridge University Press, UK. chapter Capture of CO_2. pp. 105–178.

Nair, B.K.R., Harold, M.P., 2008. Experiments and modeling of transport in composite Pd and Pd/Ag coated alumina hollow fibers. Journal of Membrane Science 311, 53–67.

Ockwig, N.W., Nenoff, T.M., 2007. Membranes for hydrogen separation. Chemical Reviews 107, 4078–4110.

Paglieri, S.N., Way, J.D., 2002. Innovations in palladium membrane research. Separation & Purification Reviews 31, 1–169.

Patil, C., van Sint Annaland, M., Kuipers, J., 2007. Fluidised bed membrane reactor for ultrapure hydrogen production via methane steam reforming: Experimental demonstration and model validation. Chemical Engineering Science 62, 2989–3007.

Peters, T.A., Stange, M., Klette, H., Bredesen, R., 2008. High pressure performance of thin Pd-23%Ag stainless steel composite membranes in water gas shift gas mixtures; influence of dilution, mass transfer and surface effects on the hydrogen flux. Journal of Membrane Science 316, 119–127.

Rothenberger, K.S., Cugini, A.V., Howard, B.H., Killmeyer, R.P., Ciocco, M.V., Morreale, B.D., Enick, R.M., Bustamante, F., Mardilovich, I.P., Ma, Y.H., 2004. High pressure hydrogen permeance of porous stainless steel coated with a thin palladium film via electroless plating. Journal of Membrane Science 244, 55–68.

Rusting, F.T., de Jong, G., Pex, P.P.A.C., Peters, J.A.J., 2001. Sealing socket and method for arranging a sealing socket to a tube. WO0163162.

Shirasaki, Y., Tsuneki, T., Ota, Y., Yasuda, I., Tachibana, S., Nakajima, H., Kobayashi, K., 2009. Development of membrane reformer system for highly efficient hydrogen production from natural gas. International Journal of Hydrogen Energy 34, 4482–4487.

Shu, J., Grandjean, B.P.A., van Neste, A., Kaliaguine, S., 1991. Catalytic palladium-based membrane reactors. A review. Canadian Journal of Chemical Engineering 69, 1036–1060.

Sieverts, A., Krumbhaar, W., 1910. Über die Löslichkeit von Gasen in Metallen und Legierungen. Berichte der deutschen chemischen Gesellschaft 43, 893–900.

Skorpa, R., Voldsund, M., Takla, M., Schnell, S.K., Bedeaux, D., Kjelstrup, S., 2012. Assessing the coupled heat and mass transport of hydrogen through a palladium membrane. Journal of Membrane Science 394-395, 131–139.

Taylor, R., Krishna, R., 1993. Multicomponent Mass Transfer. Wiley, New York.

Tiemersma, T., Patil, C., van Sint Annaland, M., Kuipers, J., 2006. Modelling of packed bed membrane reactors for autothermal production of ultrapure hydrogen. Chemical Engineering Science 61, 1602–1616.

Uemiya, S., Kude, Y., Sugino, K., Sato, N., Matsuda, T., Kikuchi, E., 1988. A palladium/porous-glass composite membrane for hydrogen separation. Chemistry Letters 17, 1687–1690.

Ward, T.L., Dao, T., 1999. Model of hydrogen permeation behavior in palladium membranes. Journal of Membrane Science 153, 211–231.

Yun, S., Oyama, S.T., 2011. Correlations in palladium membranes for hydrogen separation: A review. Journal of Membrane Science 375, 28–45.